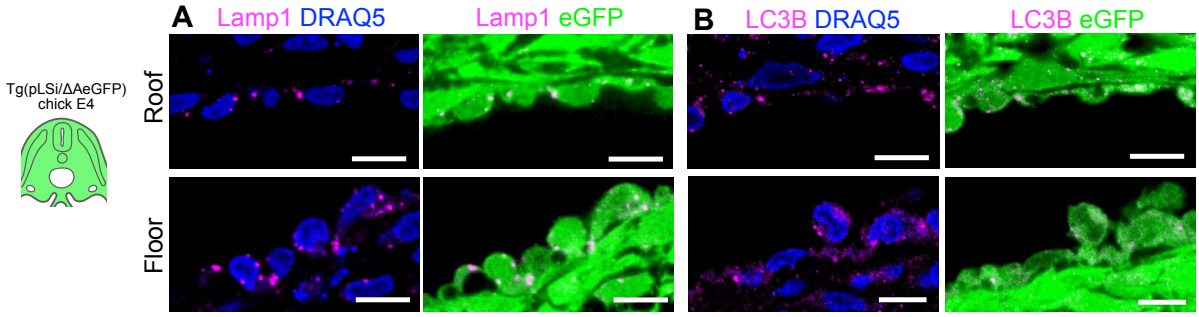

Fig. S1. Lysosome and autophagosome do not colocalize with the vacuole.
Optical cross-sections of tg(pLSiΔAeGFP) chick embryos at E4. Lamp1 (A) and LC3B (B) signals were not localized in the eGFP-negative areas. Scale bars: 10 μm.

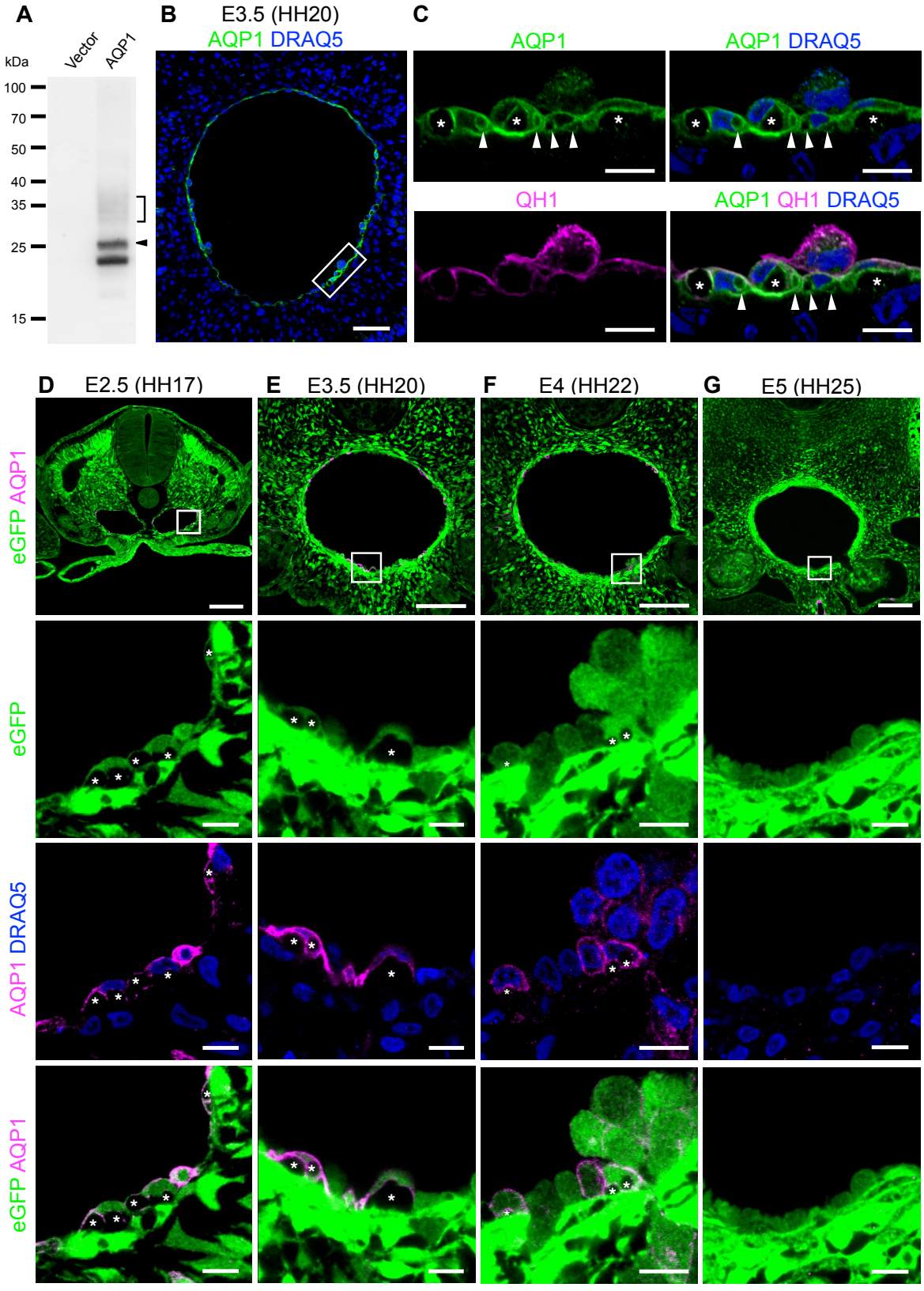

Fig. S2. AQP1 expression in the aortic endothelial cells diminishes following EHT.
(A) Western blot of pCAGGS-AQP1 transfected COS lysate using anti-quail AQP1 antibody. 28 kDa AQP1 (arrowhead) and glycosylated AQP1 (bracket) are detected. (B) Optical cross- sections of the aorta in an E3.5 quail embryo. AQP1-expressing cells are distributed in both the roof and floor of the aorta. (C) Magnified view of the rectangular areas in (B). Vacuoles/cavities are indicated by asterisks and arrowheads. AQP1 accumulated in the plasma and vacuolar membranes. The endothelial cell membrane marker QH1 overlapped with AQP1 signals in the plasma membrane. (D–G) Optical cross-sections of tg(pLSiΔAeGFP) chick embryos at E2.5 (D), 3.5 (E), 4 (F), and 5 (G). Squares indicate magnified areas in the lower three panels. AQP1 accumulated in both the plasma and vacuole membranes in the E2.5–4 aortic floor. AQP1 was not expressed in the aorta at E5, concurrent with the disappearance of vacuole/cavity-containing cells (G). Scale bars: 50 μm in (B), 10 μm in (C and lower panels in D–G), and 100 μm in the upper panels in (D–G).

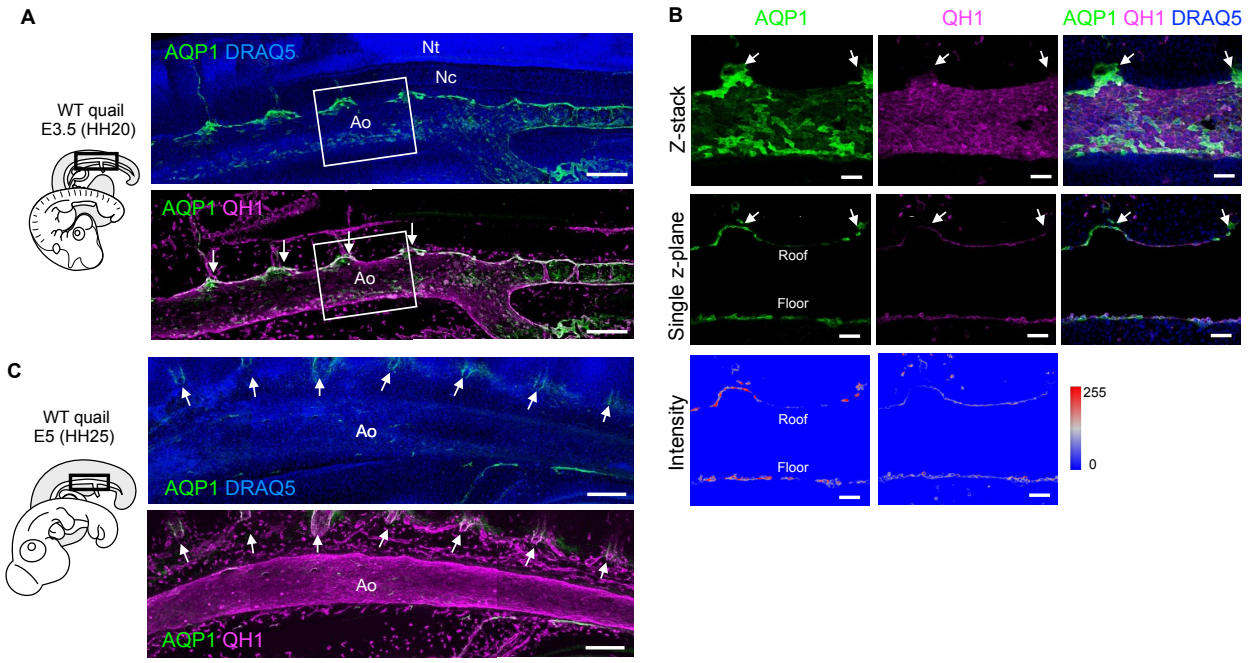

Fig. S3. AQP1 in the aorta is heterogeneous in distribution pattern and expression level.

(A and B) Z-stacked images of longitudinal optical sections of WT quail embryos at E3.5 (A) and E5 (B). AQP1^{+} cells are not uniformly distributed in the QH1^{+} endothelium of the aorta at E4 (A). AQP1^{+}/QH1^{+} intersegmental vessels (ISVs) are indicated by arrows. Only a few vascular endothelial cells expressing AQP1 are observed in the aorta at E5 (B). In contrast, endothelial cells of the ISVs express AQP1. (C) Magnified view of the rectangular areas in (A). Heat maps of AQP1 and QH1 signal intensities (lower panels) show that AQP1 is highly expressed in the endothelial cells of the aortic floor and part of the aortic roof near the intersegmental vessels (arrows in the upper two panels). Nt: neural tube, Nc: notochord, Ao: aorta. Scale bars: 200 µm in (A and B) and 50 µm in (C).

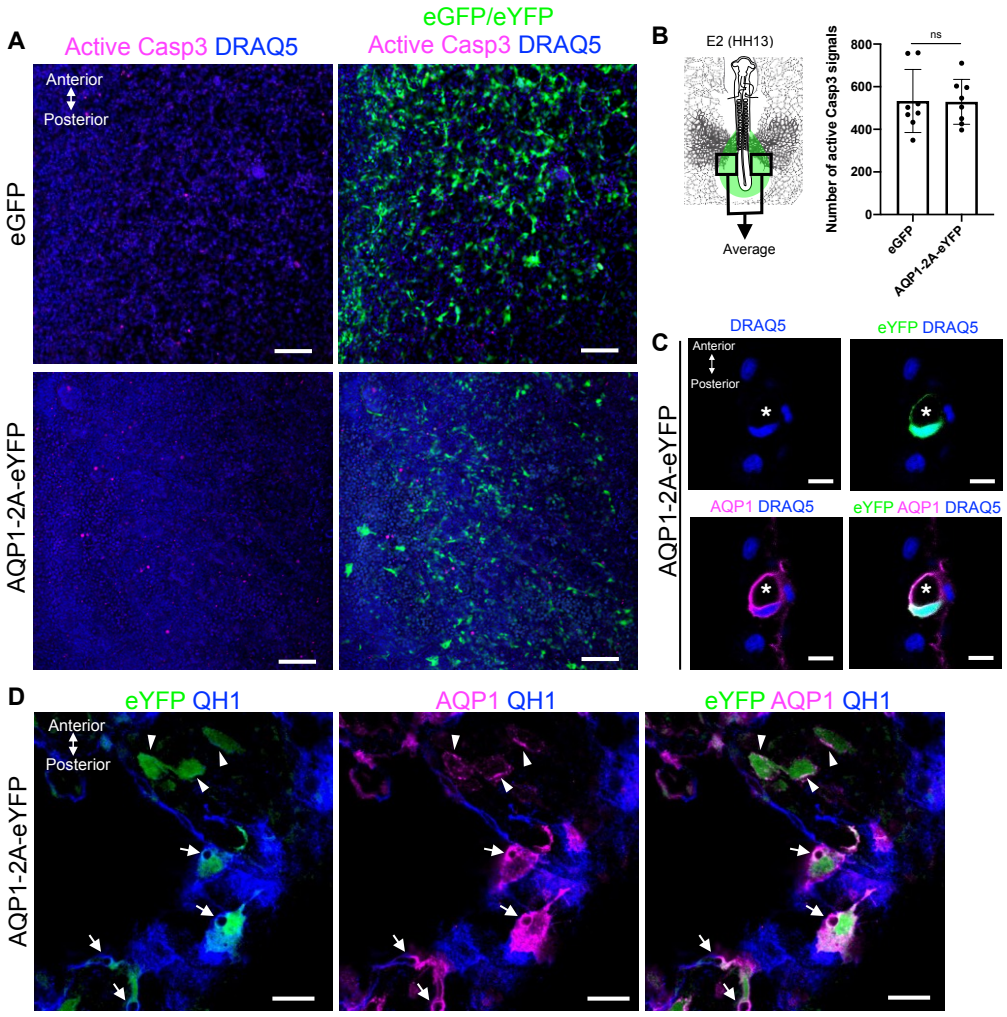

Fig. S4. Ectopic detachment of AQP1-overexpressing cells is not cell death extrusion. (A) Z-stacked images of vitelline artery regions in eGFP-(control)- and AQP1-2A-eYFP-overexpressing embryos at E2 (HH13, 28 h after electroporation). Apoptotic cells were detected through active caspase-3. (B) Average number of active caspase-3 signals on the left and right sides per embryo (n = 8) is plotted. ns: not significant by unpaired *t*-test. (C) Optical horizontal section of the vitelline artery region in an AQP1-2A-eYFP-overexpressing embryo at E2. The DRAQ5 signal represents no apoptotic or necrotic shrinkage/chromatin condensation in the nuclei of AQP1-2A-eYFP-overexpressing cells. The vacuoles are marked with an asterisk. (D) Optical horizontal section of the vitelline artery region in an AQP1-2A-eYFP-overexpressing embryo at E2. AQP1-overexpressing endothelial cells (QH1-positive) with vacuoles are indicated by arrows. Vacuoles were not found in AQP1-overexpressing non-endothelial cells (QH1-negative, arrowheads). ns: not significant, scale bars: 100 μm in (A), 10 μm in (C), and 20 μm in (D).

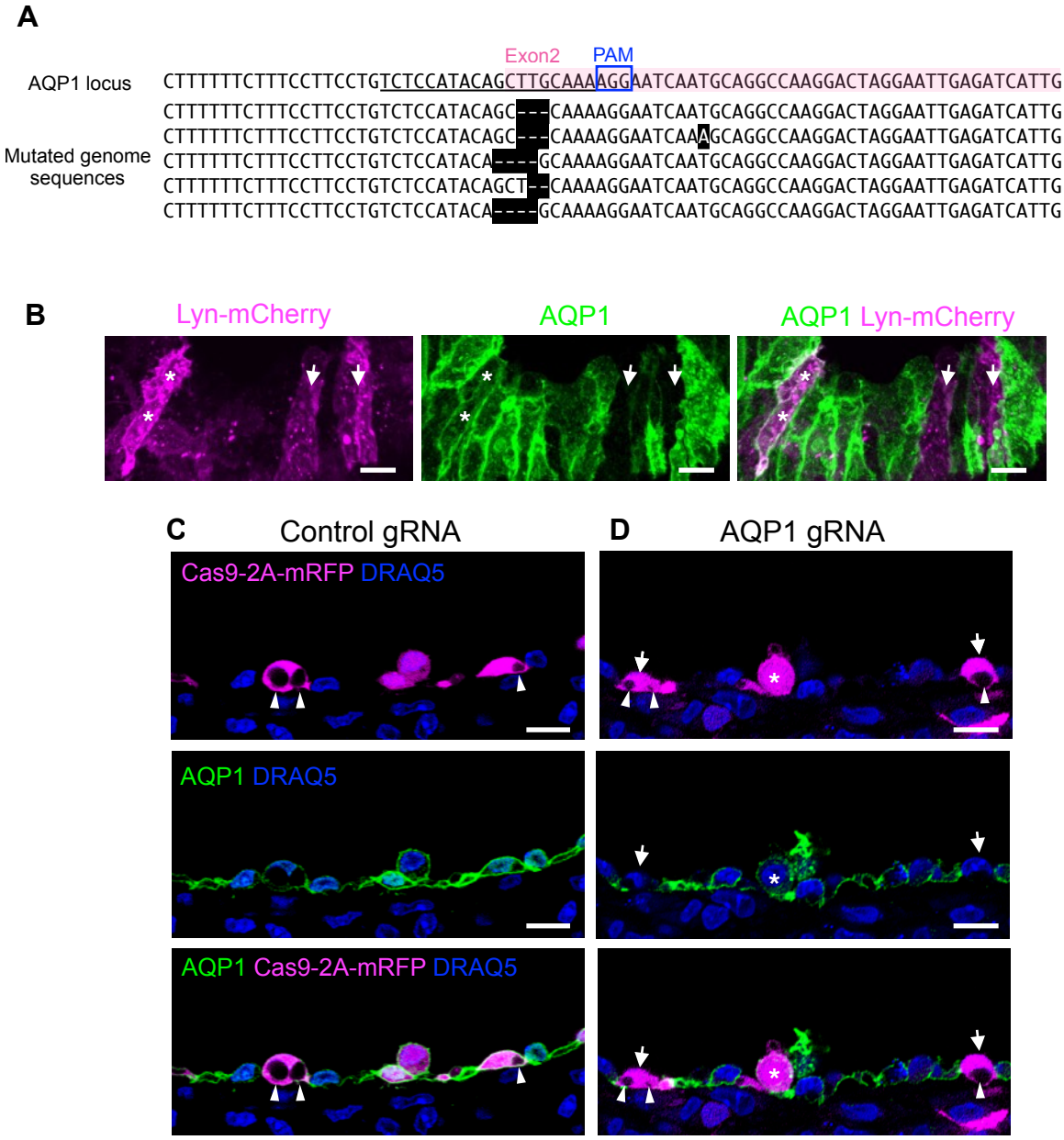

Fig. S5. *AQP1*-knockout cells become rounded with vacuoles.

(A) CRISPR/Cas9-mediated mutations in the AQP1 genome. The guide RNA (gRNA) sequence 77 is underlined. The deletions and mismatches are shaded. Loss-of-function mutations were 78 generated in the target AQP1 genome locus. (B) Oblique views of Cas9 and AQP1 gRNA79 -expressed blood vessels in quail embryo at E4. Electroporated cell membranes were labeled with co-electroporated Lyn-mCherry. The AQP1 protein was not detected in Lyn-mCherry^{+} cells

(arrows). AQP1-intact cells were also found in Lyn-mCherry^{+} cells (asterisks). These cells are considered to fail in non-homologous end-joining (Williams et al., 2018). (C and D) Optical cross-sections of aortae in control and AQP1 gRNA-electroporated embryos at E4. Electroporated cell bodies and internal vacuoles were identified by mRFP. (C) AQP1 and vacuoles (arrowheads) were not altered in control gRNA-electroporated embryos. (D) Unexpectedly, vacuoles (arrowheads) were observed in AQP1-negative cells (arrows) of AQP1 gRNA/Cas9-2A-mRFP-electroporated embryos (n = 10). AQP1-knockout cells were morphologically indistinguishable from control cells. AQP1-intact/mRFP^{+} cells are marked by asterisks. Scale bars: 10 μm.

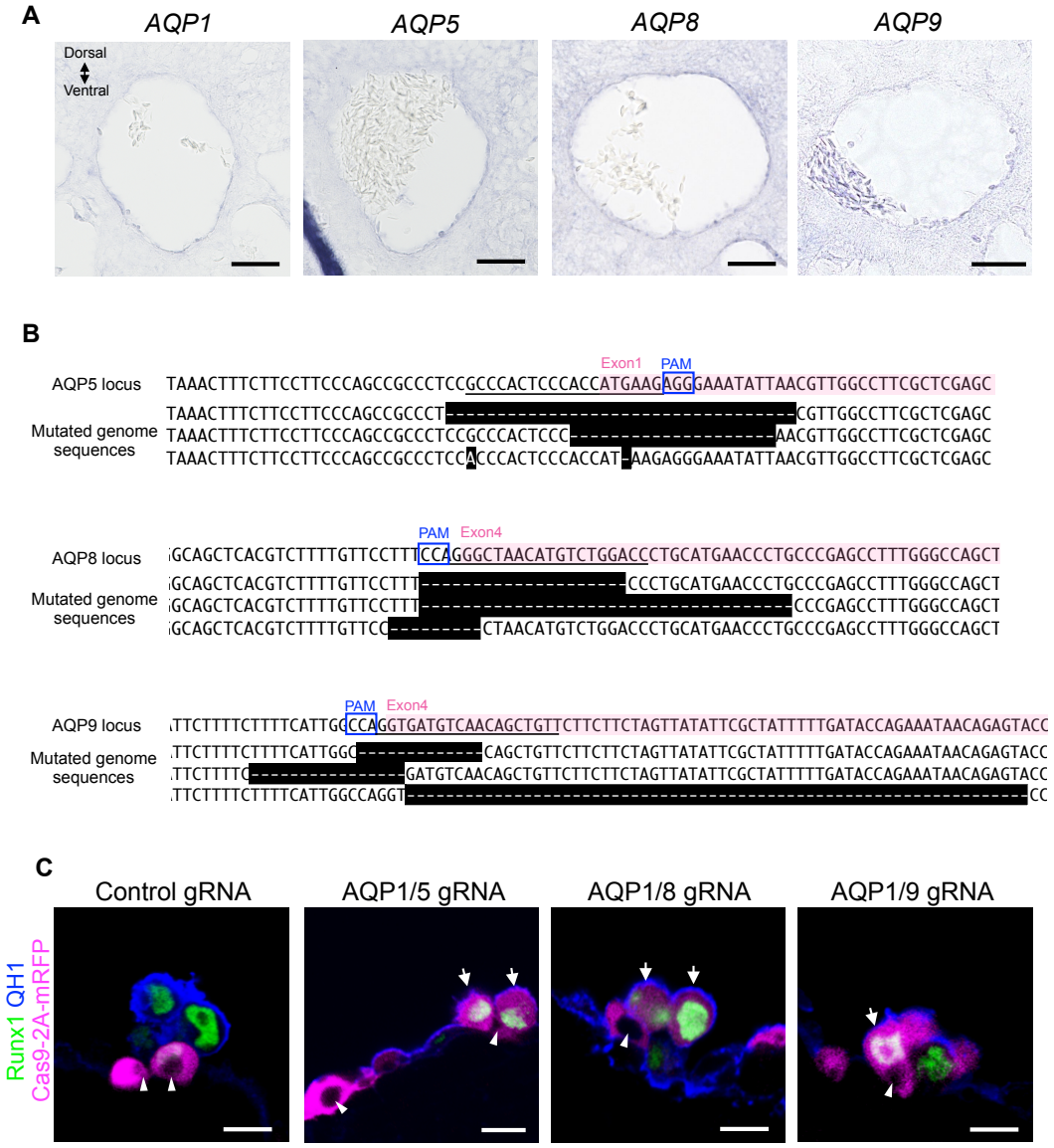

Fig. S6. AQP1, 5, 8, and 9 are redundantly expressed in the aorta.

(A) *In situ* hybridization of quail embryos at E3.5. AQP5, 8, and 9 are expressed in the aortic endothelium and surrounding mesenchyme. (B) CRISPR/Cas9-mediated mutations in genes encoding AQP5, 8, and 9. The gRNA sequences are underlined. The deletions and mismatches are shaded. Loss-of-function mutations were generated in the target AQP genome loci. (C) Optical cross-sections of aortae at E4. Electroporated cells and internal vacuoles were identified by mRFP. Vacuoles (arrowheads) were formed in AQP1/5 (n = 5), AQP1/8 (n = 5), and AQP1/9 (n = 6) double-knockout HECs (arrows). Scale bars: 50 μm in (A), 10 μm in (C).

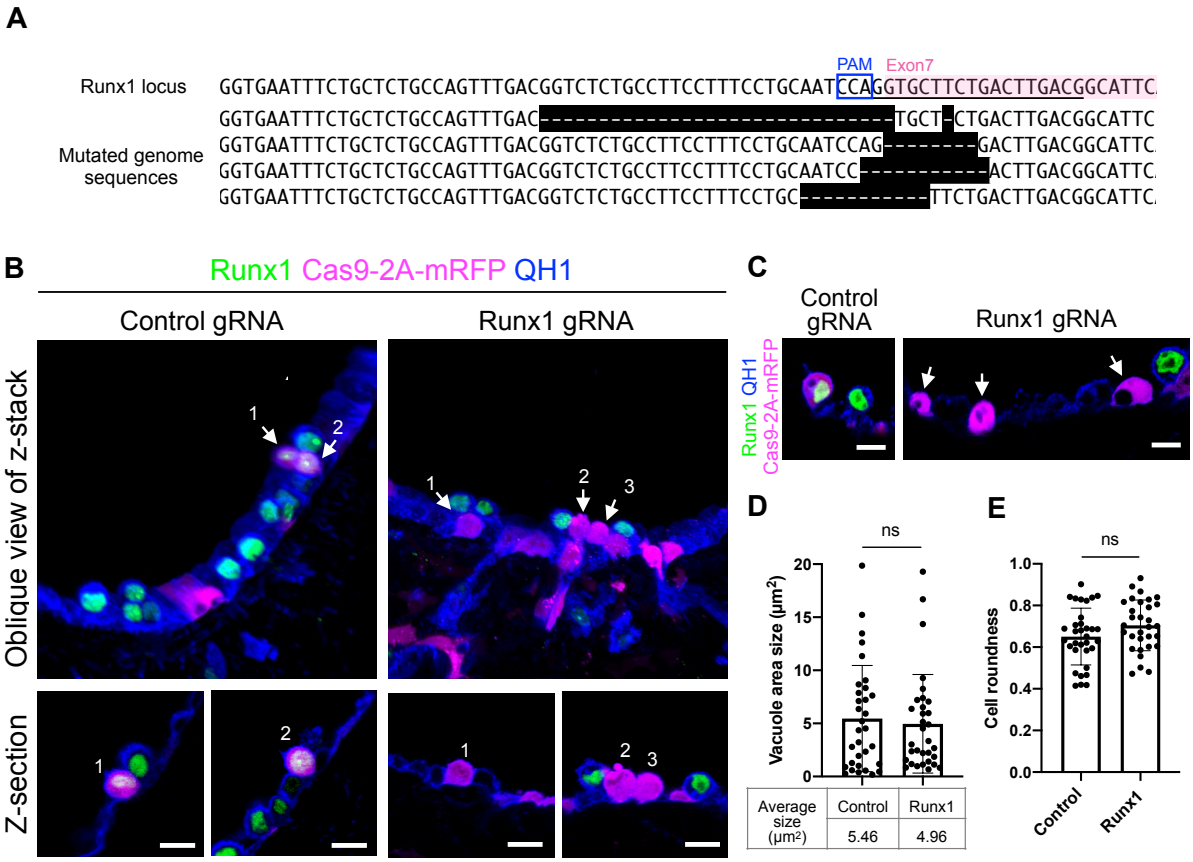

Fig. S7. Runx1-knockout does not disturb vacuole formation and cell rounding.

(A) CRISPR/Cas9-mediated mutations in genes encoding Runx1. The gRNA sequences are underlined. The deletions are shaded. Loss-of-function mutations were generated in the target Runx1 genome loci. (B) Oblique views of z-stacked images (upper panels) and optical cross- sections (lower panels) of the aortic floor at E4. Arrows in the left panel: $mRFP^{+}/Runx1^{+}$ cells in control gRNA-electroporated embryos. Arrows in the right panel: $mRFP^{+}/Runx1^{-}$ cells in Runx1 gRNA-electroporated embryos. (C) Runx1-knockout cells containing vacuoles are indicated by arrows. (D and E) No statistically significant difference in both vacuole size (D) and cell roundness (H) between control (33 slices, n = 4) and Runx1-knockout cells (31 slices, n = 4). Scale bars: 10 μm.

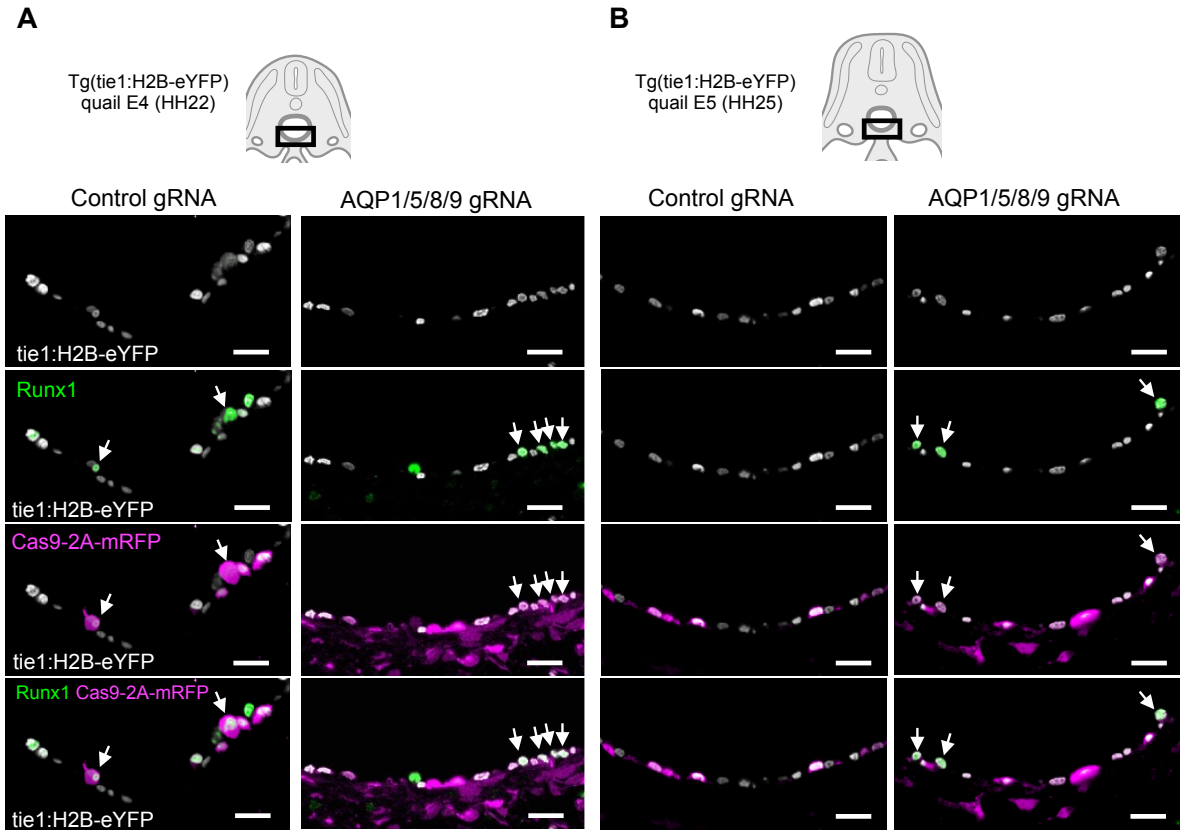

Fig. S8. Attenuation of AQP family proteins in tg(tie1:H2B-eYFP) embryos.

(A and B) Optical cross-sections of aortae in control and AQP1/5/8/9 gRNA-electroporated tg(tie1:H2B-eYFP) embryos at E4 (A) and E5 (B). The $mRFP^{+}$/$Runx1^{+}$ cells are indicated by arrows. Endothelial cell nuclei-specific eYFP signals in the tg(tie1:H2B-eYFP) embryo enabled the automatic segmentation and counting of endothelial cells and HECs. Scale bar: 20 μm.

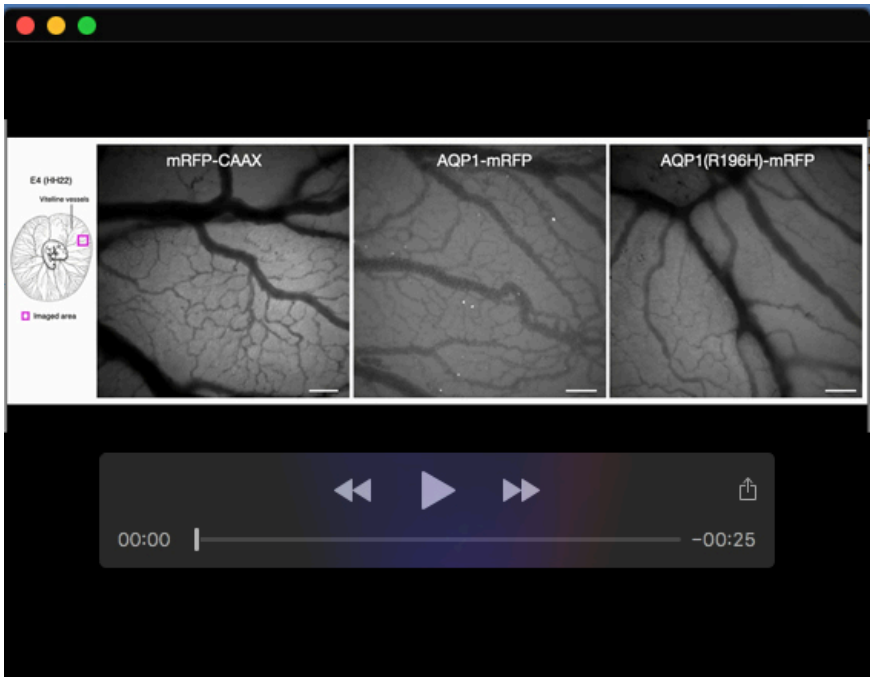

Movie 1. AQP1-overexpressing cells derived from aortic roof are found in circulation.
Video rate imaging of vitelline arteries in mRFP-CAAX, AQP1-mRFP, AQP1(R196H)-mRFP-overexpressing embryos at E4. Triple-speed replay. Scale bars: 200 µm.

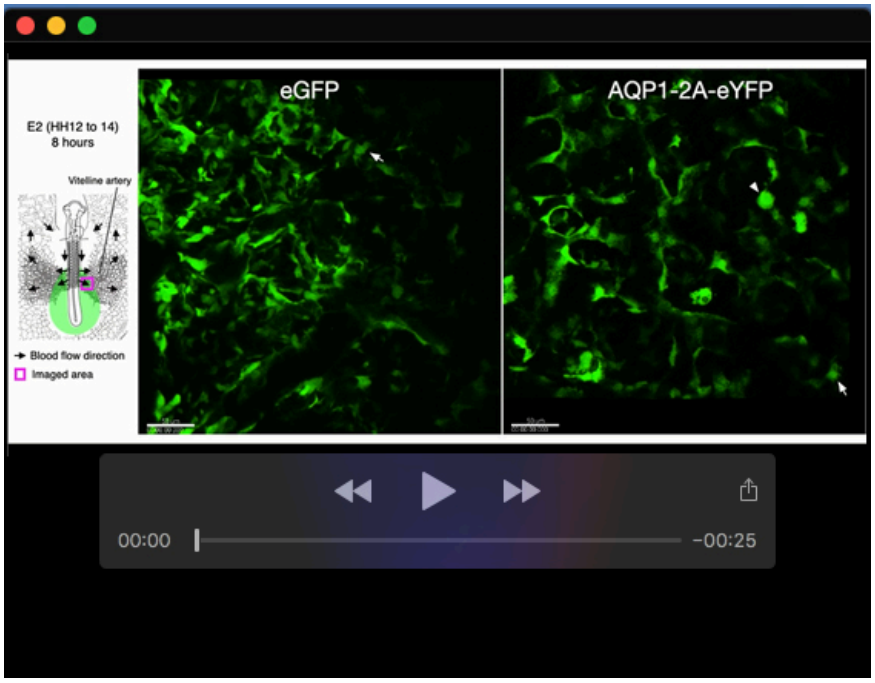

Movie 2. AQP1-overexpressing cells undergo ectopic cell rounding and detachment.
Time-lapse imaging of vitelline vessels in eGFP and AQP1-2A-eYFP-overexpressing embryos at E2. The electroporated region (colored in green), imaged area, and direction of blood flow are illustrated on the left. Freely motile rounded cells are indicated by the arrowheads. The magnified cells in Fig. 4C and Movie 3 are indicated by arrows. Scale bars: 50 µm.

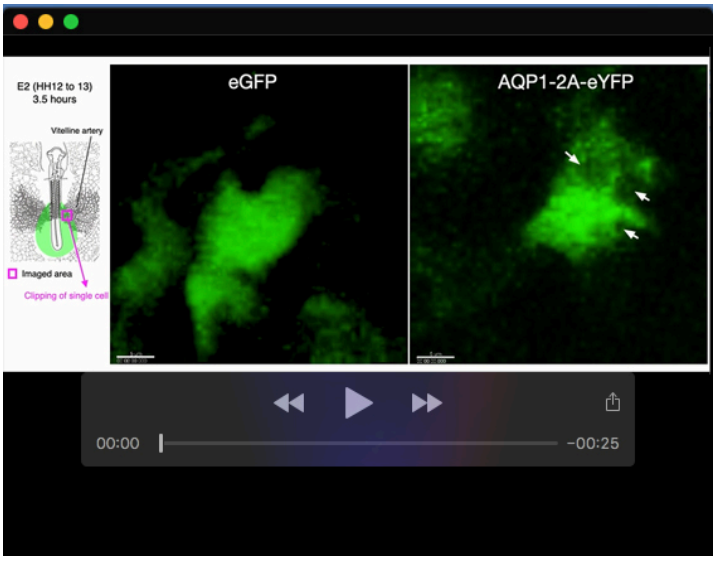

Movie 3. AQP1-overexpressing cells become rounded along with vacuole formation.
Time-lapse imaging of vitelline vessels in eGFP and AQP1-2A-eYFP-overexpressing embryos at E2. The electroporated region (colored in green) and imaged area are illustrated on the left. Ectopic vacuoles (arrows in the right panel) were formed by AQP1 overexpression, leading to ectopic cell rounding and detachment. Scale bars: 5 µm.

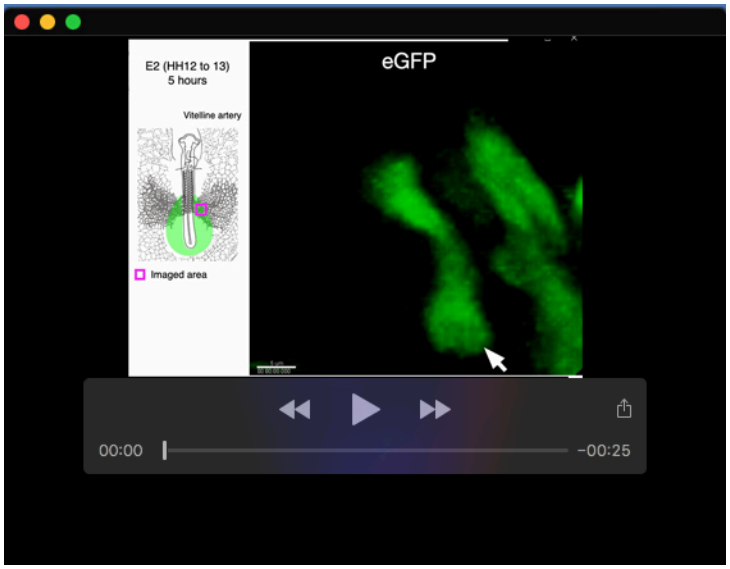

Movie 4. Dividing cell does not form vacuole during mitotic cell rounding.
Time-lapse imaging of vitelline vessels in a control eGFP-overexpressing embryo at E2. Scale bar: 5 µm.

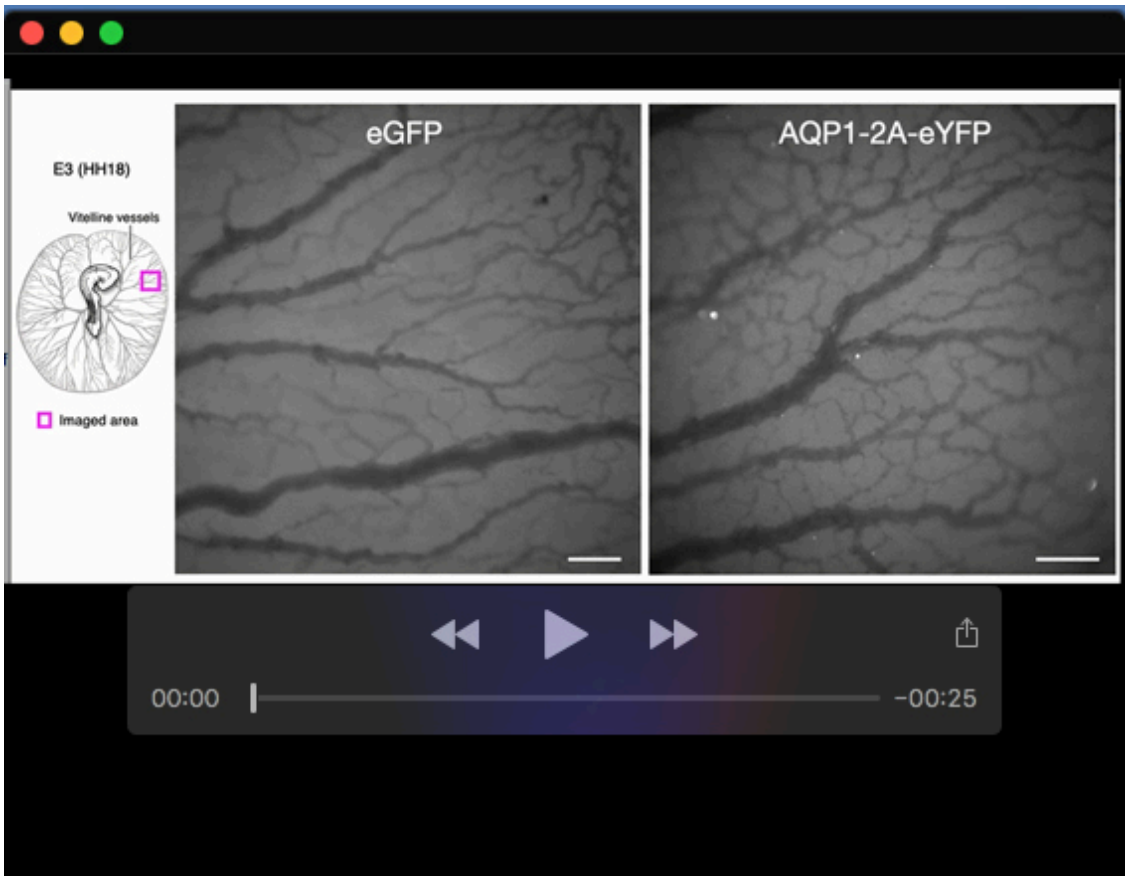

Movie 5. AQP1-overexpressing cells circulate after detachment.
Video rate imaging of peripheral vitelline arteries in eGFP- and AQP1-2A-eYFP-overexpressing embryos at E3. Triple-speed replay. Scale bars: 200 µm.